

LINEAR AND NONLINEAR MODELING OF POWER PHEMT TRANSISTORS  
WITH THE USE OF LOAD-PULL MEASUREMENTS

BY

TUAN HUU NGUYEN

BS, University of Illinois at Urbana-Champaign, 1996

THESIS

Submitted in partial fulfillment of the requirements  
for the degree of Master of Science in Electrical Engineering  
in the Graduate College of the  
University of Illinois at Urbana-Champaign, 1998

Urbana, Illinois

UIUC ID: 586-50-5782

# ACKNOWLEDGEMENTS

# ABSTRACT

## LINEAR AND NONLINEAR MODELING OF POWER PHEMT TRANSISTORS WITH THE USE OF LOAD-PULL MEASUREMENTS

Tuan Huu Nguyen, M.S.E.E.

University of Illinois at Urbana-Champaign, 1998

Supervising Professor: José Schutt-Ainé

This document describes research investigating the large-signal characterization of pseudomorphic high electron mobility transistor (pHEMTs) using load-pull measurements. The load-pull measurement is a characterization technique under large-signal conditions which determines the performance of a device under test (DUT) as the load impedance is varied. Device characteristics such as gain, output power, efficiency are examined using a passive load-pull measurement system that was assembled.

# TABLE OF CONTENTS

LIST OF FIGURES.....

LIST OF TABLES.....

## CHAPTER

<b>1</b>	<b>INTRODUCTION</b>	<b>1</b>
1.1	Foreword.....	1
1.2	Load-Pull Measurement Technique.....	
1.3	Modeling.....	
1.4	Overview of this Thesis.....	
<b>2</b>	<b>BACKGROUND</b>	<b>5</b>
2.1	Introduction.....	
2.2	Principle of a Load-Pull System.....	
2.3	Passive vs. Active Load-Pull Systems.....	
2.3.1	The Active Load-Pull Technique .....	
2.3.2	The Passive Load-Pull Technique.....	
2.4	Tuner Description.....	
2.5	Load-Pull Contour Theory .....	
<b>3</b>	<b>THE MEASUREMENT SYSTEM</b>	<b>13</b>
3.1	Introduction .....	
3.2	System Description.....	
3.3	System Calibration.....	
3.3.1	Tuner Network Calibration.....	
3.3.2	Probe Network Calibration.....	
3.3.3	Overall System Calibration.....	
3.4	Accuracy Considerations.....	
3.5	Measurement Procedure.....	

3.6	Future Improvements.....	
<b>4</b>	<b>MODELING AND EXTRACTION PROCEDURES</b>	<b>30</b>
4.1	Introduction.....	
4.2	Small-Signal Modeling.....	
4.1.1	Equivalent Circuit.....	
4.2.2	Model Parameter Extraction.....	
4.2.3	Optimization Results.....	
4.2	Large-Signal Modeling.....	
4.1.1	DC I-V Nonlinear Parameter Extraction.....	
4.1.2	Optimization Results.....	
<b>5</b>	<b>LOAD-PULL MEASUREMENTS AND SIMULATION DATA</b>	<b>40</b>
5.1	Introduction.....	
5.2	Load-Pull Measurement Data.....	
5.3	Load-Pull Simulation.....	
5.4	Comparisons.....	
<b>6</b>	<b>CONCLUSIONS</b>	<b>47</b>
6.1	Summary .....	
6.2	Conclusions .....	
6.3	Suggestions For Continued Research .....	
<b>APPENDIX</b>		
A.1	Load-Pull Measurement Data .....	
<b>LIST OF REFERENCES.....</b>		

## LIST OF TABLES

## LIST OF FIGURES

2.1	Basic block diagram of a load-pull measurement system. ....	.....
2.2	Simple network for describing the active load-pull measurement concept. The equivalent load impedance is separately denoted by the dotted lines.....	.....
2.3	Block diagram of a passive load-pull system .....	.....
2.4	Basic operation of the Focus electromechanical tuner used. $ \Gamma_{\text{TUNER}} $ is controlled by the slug insertion depth shown in (a). The phase of $\Gamma_{\text{TUNER}}$ is varied by changing the distance, $l_{\text{PHASE}}$ , from the reference plane, as shown in (b). An equivalent circuit for the tuner is drawn in (c). ....	.....
2.5	Signal flow-graph for the electromechanical tuner .....	.....
3.1	RF block diagram of the millimeter-wave passive load-pull measurement system .....	.....
3.2	Illustration of (a) the tuner network calibration setup and (b) the probe network calibration setup .....	.....
3.3	Example of a tuner network calibration at (a) 26.0 GHz and (b) 24.5 GHz. The locus of the 360 calibration points are evenly spaced on the Smith chart for (a), but are absent in the low-directivity area in (b).	.....
4.1	Small-signal pHEMT equivalent circuit model .....	.....
4.2	Measured vs. modeled S-parameter plots .....	.....
4.3	Equivalent circuit model of the modified Materka's large-signal MESFET model .....	.....
4.4	MDS representation of the nonlinear currents in the nonlinear circuit model .....	.....
4.5	DC I-V plots of the measured vs. calculated device currents with respect to bias voltages. (a) $I_{\text{GD}}$ vs. $V_{\text{DS}}$ (b) .....	.....
4.6	Comparison of S-parameters for the nonlinear model vs. the linear model. ....	.....
5.1	Calibration data plots for (a) the source tuner network and (b) the load tuner network 26.0 GHz.	.....

- 5.2 Calibration data plots for (a) the input network and (b) the output network at 26.0 GHz. The networks consist of the mathematical combination of the tuner network calibration data with the probe network calibration data.
- 5.3 Output power levels at 26.0 GHz vs. input power while the load is kept at the optimum. (a)
- 5.4 Load-pull measurement data in the output impedance-plane. Contours of constant output power at 26.0 GHz and 11.6 dBm input drive are shown for a 300  $\mu\text{m}$  pHEMT. The input reflection coefficient used for the device was .
- 5.5 Load-pull modeled data in the output impedance-plane using MDS. Contours of constant output power at 26.0 GHz and 11.6 dBm input drive are shown. The input reflection coefficient used for the device was .



# CHAPTER 1

## INTRODUCTION

### 1.1 Foreward

Most microwave designers should be very familiar with the use of S-parameters for the design of small signal amplifiers. However, small signal S-parameters are useless when designing or troubleshooting power amplifier circuits where the transistor is operated under its nonlinear mode or in a mode other than Class A. Also because the power delivered by a power FET is strongly dependent on the load impedance presented to the device, the knowledge of the optimum load impedance is a very important piece of information for circuit designers. Thus, it is often-times necessary to measure the load impedance under the actual operating conditions for a device. This type of measurement has classically been referred to as a load-pull measurement. Load-pull measurements of nonlinear active two-port networks is well known as being a useful technique for characterizing the large-signal properties of microwave transistors.

### 1.2 Motivation

As part of this thesis, in conjunction with the needs of Raytheon's MMIC Modeling Group, a millimeter-wave load-pull system was constructed. The measurement test bench will be used to verify and support the various models

created by modeling team. The automated measurement system will be described in this thesis.

In the ever-increasing development in today's communication systems, solid state power amplifiers are becoming more and more used. With the use of power amplifiers in any communication link, it is important to examine the performances of output amplifiers in terms of power added efficiency and intermodulation. Improving the trade-offs between these features is critical with the design of multicarrier amplifiers. Large signal measurement systems provide valuable information in designing optimized communication power amplifiers. A load-pull measurement system help achieve that task.

The design of microwave solid-state power amplifiers is still largely based on small-signal characterization of power transistors [Cusack], because large-signal modeling of power transistors may not be accurate enough to be used in the design of solid-state amplifiers, especially when working at millimeter-wave frequencies.

The characteristics of a pseudomorphic high-electron mobility transistor (pHEMT) are examined in this research. The device was chosen to be modeled and measured for its large-signal properties because of its more prevalent usage in many microwave circuit applications. Power pHEMTs exhibit high-power handling and power-added efficiencies (PAE), capable of providing both power and low noise amplification with applications ranging from L-band to millimeter wave. These include low-noise amplifiers (LNAs), as well as high-efficiency power amplifiers for both receive and transmit modules for high-performance radar and communications satellites.

Since the first microwave GaAs MESFETs were reported in the early 1970's, they have been used extensively for providing small-signal amplification at frequencies above 1 GHz. The development of GaAs MESFET power amplifiers, however, have been less dramatic; devices operating in the non-linear region are difficult to characterize and designs are consequently far from exact and optimal. [Pierpoint]

The emphasis of this thesis was upon the development of a high frequency power measurement system capable of generating constant output power circles.

### **1.3 Overview of this Thesis**

This thesis describes work carried out on the large-signal modeling and characterization of a 300  $\mu\text{m}$  4-finger power pHEMT and the automated measurement of its load-pull behavior at millimeter-wave frequencies. The object is to facilitate the design of power amplifiers with power, gain, bandwidth, and efficiency as design parameters. Large-signal characterization of the device was accomplished with the use of small-signal, pulsed I-V, and load-pull measurements at 26.0 Ghz. Pertinant information about the load-pull measurement technique are provided in Chapter 2. Chapter 3 describes the system hardware and measurement technique used to charcterization the device. A small-signal and large-signal model for the device was developed in the frequency range of 1.0 GHz to 50.0 GHz. The modeling techniques are discussed in Chapter 4. Experimental and modeling results of the large-signal characterization of the pHEMT device are presented and

examined in Chapter 5. Chapter 6 contains a summary of the work accomplished along with suggestions for continued research.

## CHAPTER 2

# BACKGROUND

### 2.1 Introduction

In the design of microwave power amplifiers, the knowledge of the optimum load impedance is generally required to match the device to other parts of the circuit. The problem with designers is that the load impedance is a function of output power. With small-signal amplifiers, it is often possible to accurately model and predict the optimum source and load impedance. With large-signal amplifiers, however, it is unpredictable to estimate how the load impedance varies with the output. As a result, the use of small-signal S-parameters has little relevance with the design of large-signal amplifiers and large-signal characterization techniques must be used. Load-pull measurements provide the ability to measure characteristics of a device under test (DUT) under realistic operating conditions. In the measurement, the main independent parameter is not frequency, power, or bias, but the source or load impedance at the fundamental frequency presented to the DUT.

There a variety of uses for a load-pull measurement system. As stated earlier, it is capable of measuring the optimum source and load impedance required to obtain the maximum output power from a given device at millimeter-wave frequencies. It can also be used to determine the load sensitivity on a given device and various useful parameters for a designer such as power added efficiency (PAE),

power gain, and power-output contours. A load-pull measurement system can also be capable of testing a device for its harmonic performance by examining a device's inter-modulation distortion (IMD) and third-order intercept (TOI) point. Many industrial companies also use a load-pull to verify and support equivalent-circuit linear and nonlinear models of GaAs devices. Load-pull measurements can be used for both linear and nonlinear devices, although it is most useful and mainly used for large-signal measurements when the device is operated in a nonlinear fashion.

One of the important results that a load-pull measurement can provide is a series of constant output power contours plotted on a Smith Chart. Each one of these contours represents the range and values of the load terminations necessary for a device to produce a given output power with a predetermined input power, frequency, and bias conditions. A separate load-pull measurement has to be taken at each power level and frequency of interest because the load contours are generally very sensitive to these variables for most high power devices and oscillators.

## **2.2 Principle of a Load-Pull System**

The basic idea of a load-pull measurement consists of presenting a known load and source impedance to a device under test at a given frequency and then measuring the associated input power, output power, reflection coefficients, and dc bias conditions.[x1] A basic block diagram of the system is expressed in Figure 2.1. Measurements are made as a function of the input power level and device terminations. The impedances of the device terminations are the key variable in this type of measurement.

The impedance measurement can be accomplished with a dual directional coupler reflectometer.

As the source and load impedances are varied, device characteristics such as output power gain will change accordingly.

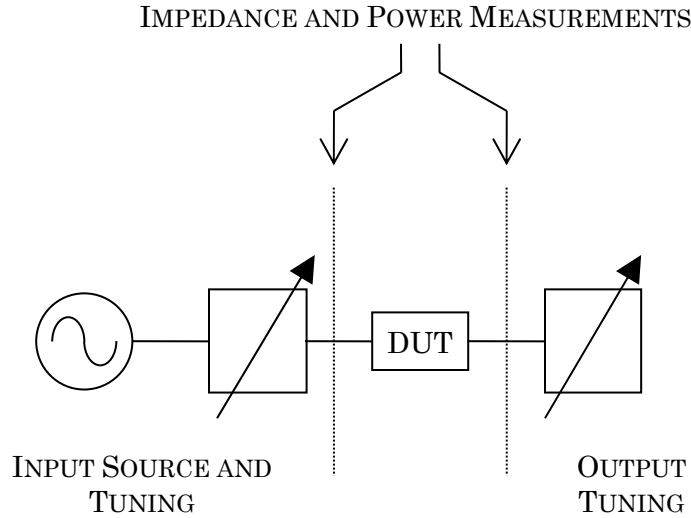


**Figure 2.1.** *Basic block diagram of a load-pull measurement system.*

### 2.3 Passive vs. Active Load-Pull Systems

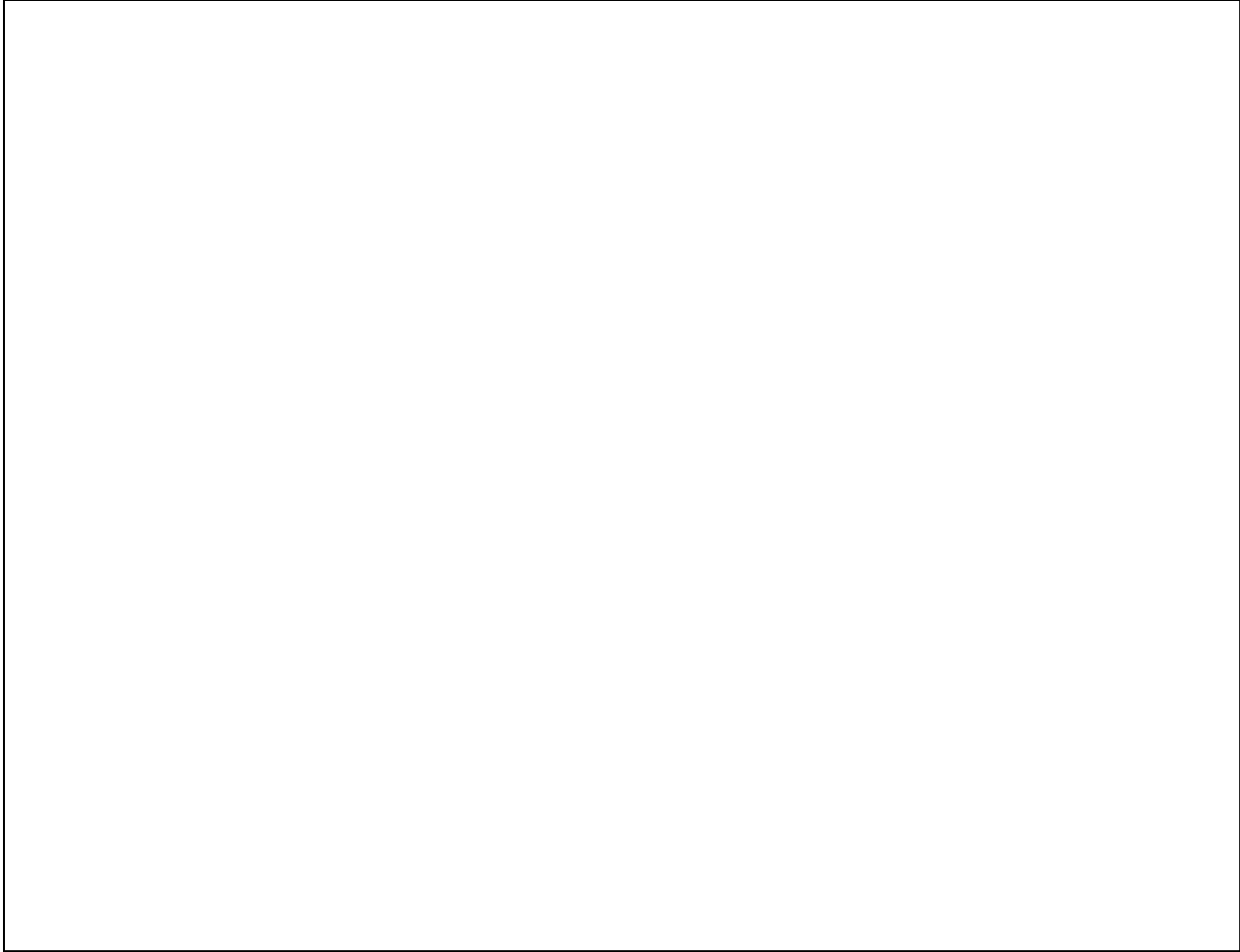
There are essentially two main techniques used to perform large signal measurements of nonlinear microwave devices. The difference between the two ways of implementing a load-pull measurement systems lies in how the load impedance is generated. Conventional load-pull measurements, including the system discussed in this thesis, generally requires impedance-transforming tuners to provide a suitable range of output load impedances to the device under test. The

tuners are usually electro-mechanical, using a “sliding slug” to achieve the variable load conditions, and will be discussed in greater detail later in this chapter. This method is commonly referred to as the passive load-pull technique. The second method relies on an electronic simulation of loads by simultaneously driving each port on the DUT with coherent incident power waves. This technique, known as the active load-pull technique, was initially investigated by Takayama in 1974 [1]. The active load-pull system will be briefly explained to give the reader some insight about the technique, but more emphasis will be placed upon the passive load-pull technique, as it was the type of system that was constructed.

### **2.3.1 The Active Load-Pull Technique**

This active load-pull system provides an equivalent load-pull measurement technique without the use of an output impedance tuner. It can be used if it is necessary to tune to the outside of the Smith chart. The output load impedance is defined and varied using boundary conditions between the incident and reflected power waves at the transistor output port. Figure 2.2 gives the basic block diagram of an active load-pull setup to help explain the principle. This system makes use of two coherent RF signals simultaneously injected into the input and output ports the transistor under test, where the amplitude and phase of the signal entering the output port is varied. The input signal determines the operating drive level, while the phase and amplitude of the injected signal establish the equivalent output load





impedance of the device. The amplitude and phase of the “reflected” signal entering the output of the DUT can be adjusted with the use of an amplifier, an attenuator, a phase shifter, and either a circulator or a high directivity directional coupler. The output load impedance is defined and varied using boundary conditions between the incident and reflected power waves at the transistor output port. With this system, it is theoretically possible to synthesize any load impedance, but also large incident power waves driving the output port of the DUT are required. One consideration to take into account with the active tuning system is the to carefully monitor the phase of the injected power wave at the transistor output port. If the phase is not properly

controlled, the system may be potentially unstable if 180 degrees of phase shift and a gain of 1 is achieved around the path from the input to the output of the amplifier in the tuner. Thus damage to the device may occur.

### **2.3.2 The Passive Load-Pull Technique**

The passive load-pull technique, as stated earlier, relies on the use of passive tuners to adjust the reflection coefficient of the signal incident upon the output of the device. Theoretically with the absence of losses within the system, simulation of any passive impedance on the Smith chart can be achieved. Tuner measurements have been investigated from the beginning of microwave technology, however it was not possible to extract the impedance conditions during the actual measurement until the mid 1970's, where the first automatic load-pull system was designed and assembled at RCA David Sarnoff Research Laboratory in New Jersey [1]. It was possible to compute the impedance of the tuners as a function of their geometry and position. Other laboratories have also developed and published semi-automatic or automatic tuner systems, but RCA's was the first to commercialize their system in the early 1980's.

The use of manual tuners for load-pull measurements has often been questioned in the past because of both the heavy experimental procedures and in the reproducibility of data. In order to improve the measurement speed and to make it easier to obtain repeatable data, [Sechi 83] proposed an automatic test set based on motorized passive tuners and on an automatic curve-tracking algorithm, based on a previously characterized load model.

One limitation that may be encountered with the use of a mechanical tuning systems is the ability to achieve highly reflected loads close to the edge of the Smith chart. This is due to the inherent losses of such devices.

**FIGURE 2.3:** *Block diagram of a passive load-pull system*

## 2.4 Tuner Description

The tuner that was used in this project is an electromechanical instrument designed to operate over a frequency range of 18 - 40 GHz. It uses computer-controlled stepper motors to allow for the positioning of probes, creating repeatable input and output microwave reflection coefficients. The tuner, produced by Focus Microwaves, consists of a slug inserted into a slotted coaxial transmission line to create the necessary input and output impedances, as is illustrated in Figure 3.2. It is based on a length of  $50 \Omega$  slab-line which has an open structure allowing the insertion of a small metallic slug. As the slug is inserted into the slotted line, a shunt reactance between the outer and inner conductor is created. The magnitude of the reflection coefficient observed looking into the tuner is varied with the insertion depth; increasing the insertion depth,  $d$ , of the slug increased the  $|G_{TUNER}|$ . To adjust the phase of the reflection coefficient,  $l_{PHASE}$ , the distance from tuner reference plane to the slug is varied on the slotted line. Stepper motors allow

for both the horizontal and vertical movement and are controlled with the use of a tuner controller card and by software produced and developed by Focus Microwaves.

With the use of electromechanical tuners in a load-pull system, there is an inherent finite amount of loss incurred within the system. Specifically the losses of the tuners must be examined. If there is a large amount of loss in the signal path, high reflection coefficients near the edges of the Smith chart may not be attainable when making measurements. An expression for the loss caused by the tuner may be derived from a consideration of the signal flow graph in Figure XX. The tuner loss ranges from XX dB for the very high reflection coefficients with the slug fully inserted to  $< 0.1$  dB when the slug is fully withdrawn. [Pierpoint]

**FIGURE 2.4:** *Diagram of the focus electromechanical tuner (1 pg.)*

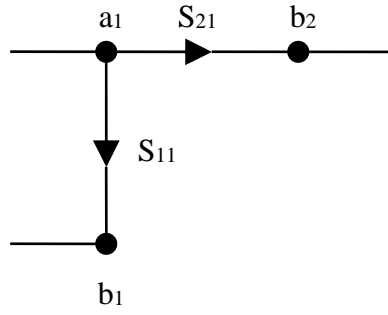


**Figure 2.5:** *Signal Flow-Graph for the Electromechanical Tuner*

$$Loss = \frac{P_o}{P_i} = \frac{|S_{21}|^2}{1 - |S_{11}|^2} \quad (2.1)$$

## 2.5 Load-Pull Contour Theory

One of the results that a load-pull measurement can provide are a set of power contours. The contours are a loci of load (or source) impedances of constant output power on the Smith chart for the given test condition. For small-signal, the contours are circular and can be computed from the S-parameters of the device. As the device operates further in its nonlinear mode, the contours deviate further from appearing circular. Load-pull contours, as they are commonly referred to, are often inaccurate or difficult to compute and simulate with nonlinear commercial simulators, such as HP-Eesof's Libra, HP's MDS, or Compact's Harmonica. The simulation of the contours depend on the accuracy of the nonlinear model, where the models generally are only valid for light gain compression only. At 2 or 3 gain compression, the results provided by nonlinear models are usually inaccurate. Thus there is a need for load-pull measurement systems in the industry to generate accurate load-pull contours.

Load-pull contours provide a microwave designer useful information of the measured device under test with the knowledge of the appropriate load impedance for a desired output power or gain. It would then be possible to design an output matching circuit by matching to the appropriate impedance point indicated by the load-pull data. The data also indicates to the designer how sensitive the output power of the device is to various load impedances. An input match can also be designed using the appropriate input impedance information from the use of the input tuner.

## **CHAPTER 3**

### **THE MEASUREMENT SYSTEM**

#### **3.1 Introduction**

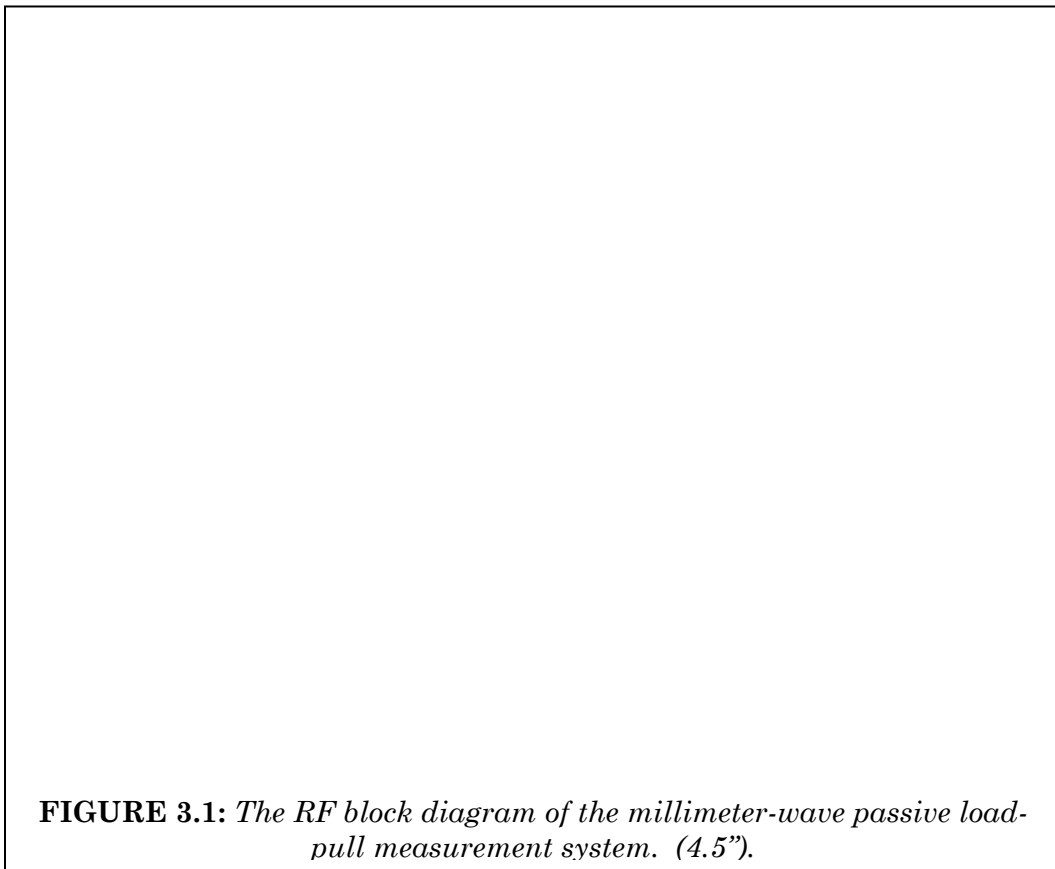
While Chapter II explained the theory and the uses of a load-pull system, this chapter will give a detailed description of the actual system used. For this thesis, an automated passive load-pull system using a commercial computer controlled tuners (Focus Microwaves [x3]) was assembled to make large-signal measurements in the millimeter-wave frequencies. Because of the frequency limitations of the components, the system was only capable of performing large-signal characterizations of devices between 24 to 31 GHz. The results and measurements taken using the system will be presented in Chapter VI, along with the modeled data.

#### **3.2 System Description**

A fairly straight forward, passive load-pull system using electromechanical tuners was assembled for this thesis. A block diagram of the load-pull measurement setup is shown in Figure 3.1. The setup, as stated in the previous chapter, consists of five main sections: the input source, the input and output tuner assemblies, the DUT assembly, and the measurement instruments. The input source is comprised of a signal generator ---. A high power traveling wave tube (TWT) amplifier is



connected to the signal source to produce the high level input power necessary for the measurement of power transistors. The input and output tuning assemblies both contain a coupler, isolator, bias tee, along with the tuner to create the desired reflection coefficients. Isolators are used both the input and output tuning assemblies to create a nominal 50 ohm match and to separate VSWR changes in the transmitting signal.



The pHEMT device was tested using an Electro-Glas on-wafer probe station. Because the system was designed for measurements to be taken at millimeter-wave frequencies, an on-wafer setup was used for the DUT to minimize the amount of loss and eliminate as many parasitic effects as possible. Four-inch low-loss cables were

used to connect the tuners to the cascade probe tips on the probe station. Cables were used instead of waveguide connectors in the system to provide some flexibility in the maneuvering of the placement of the probe tips, where the tuner assemblies were fixed. Skin effect was a concern with the use of coaxial cables at the high frequencies, but both cables were tested to have approximately 0.5 dB of return loss with an insertion loss of greater than 20 dB between 24 and 31 GHz using an HP8510C Network Analyzer.

In order to obtain high-reflection coefficients with the use of the mechanical tuners in the passive load-pull technique, the loss introduced between the tuning sections and the device must be minimized. [Ferrero 94] refute that passive tuning structures may be unsuitable for on-wafer device measurements, but it will be shown with the system described in this thesis and from the results of the measurements that it may be suitable.

A vector network analyzer is not needed for each measurement but only to calibrate the tuners and the setup initially and subsequently for any periodic recalibration.

### **3.3 System Calibration**

The calibration procedure for the load-pull measurement system consists of a two-tier calibration process using the HP8510C Network Analyzer and Focus's CCMT software. "Two-tier" refers to the mathematical combination of two independent calibration files, namely the tuner network calibration and the probe network calibration. The network analyzer with the measurement cables is

manually calibrated over the broadband frequency range of interest prior to each tuner and probe network calibration procedure. Then each tuner assembly, which involves the tuner, bias tee, isolator, and directional coupler, is characterized so that that the incident power on the device and the measured power at the output may be corrected for losses. Finally, the on-wafer setup, which included both tuner assemblies, the probe cables, and probe tips, was characterized in the two-tier calibration process. The input and output power, frequency, and bias are then recorded at each point in turn.

A network analyzer cable calibration was manually performed prior to the actual load-pull system calibration. This involved a standard TRL calibration using 2.92 mm connectors. Because of the flexibility and variability of the cables, this step must be done with the utmost precision and minimal movement of the cables as possible. A five to ten minute "rest" period was needed between measurements for the cables to settle down, thus minimizing variability in the cables and improving the repeatability of future calibrated measurements. It was found that measurement values using the cables were imprecise and drifted during the first five minutes after terminations were attached.

The first step of the actual load-pull calibration procedure involves individually calibrating both the input and output tuning assemblies using the CCMT software. With the input tuner assembly attached to the network analyzer and computer controller, the CCMT software stepped through 360 discrete reflection coefficients on the Smith chart. This was performed by first varying the depth of the slug and then varying the position of the slug along the air line as described earlier. The computer then records the exact position of the slug along with its associated

reflection coefficient from the network analyzer and associated losses through the system.

For a given frequency, the 360 discrete calibration measurements could then be plotted on the Smith chart using the CCMT software. A calibration was deemed acceptable if the calibration points were spaced fairly evenly apart and a maximum reflection greater than 0.85 was obtainable. Also, a good calibration should be able to reach most areas of the Smith chart, including the center of the Smith chart (at  $Z = 50 \Omega$ ). Any such absence represents a mismatch in one of the components of the tuner assembly or a significant amount of signal loss through the network. Impedance mismatches, which can be caused by the bias tee, prevent true match from being obtained in the network. Also, at certain frequencies, the isolator may have difficulties in producing a low return loss. Thus the calibration circle of points may appear to be offset from the center or a lack of calibration points in the low-directivity area on the Smith chart may occur. Figure 3.2 (a) depicts the calibration performed at 26.0 GHz that will be used for the load-pull measurements in this thesis. Figure 3.2 (b) shows an example of a calibration measurement at 24.5 GHz, a frequency where it is apparent that accurate load-pull measurements would not be possible. After calibration is deemed acceptable, a calibration file for each frequency containing the electrical performance of the network was saved onto the computer. This process was repeated for both the input and output tuner networks.

The next procedure calibrates the probe network, which consists of the probe tips and probe coaxial cables. This calibration is similar to that used on a standard network analyzer. Again a network analyzer cable calibration was performed prior to the procedure. Using the CCMT software, a standard TRL calibration was

performed using on-wafer standards. The standards were constructed on the substrate to reproduce the de-embedding planes of reference. The calibration procedure was then verified by measuring a short. After verification, the software translates the probe network calibration data into a two-port S-parameter data file.

Error coefficients from the tuner network calibration are then cascaded with the S-parameter data file from the probe network calibration to achieve an overall system calibration file. The overall system calibration data points were plotted on a Smith chart and is displayed on Figure 3.3. For the measurements that were taken at 26.0 GHz, a maximum reflection coefficient of 0.75 was obtainable. It is preferable to be able to achieve high reflection coefficients in a load-pull measurement system, preferably with a reflection coefficient greater than 0.8, because optimum source impedances for maximum power of GaAs transistors are generally high reflect impedances.

### **3.4 Accuracy Considerations**

The accuracy of the load-pull impedance measurement will be limited and should be comparable to the accuracy of the HP 8510C Network Analyzer used in a manual mode at a single frequency.

### **3.5 Measurement Procedure**

Using Focus's CCMT software, the measurement system can automatically sweep through a selected range of device biases, input power levels, frequencies, and

output load impedances to generate constant output power and efficiency contours. Automatic operation involves changing the stepper-motor positions to repeat the exact points at which the input or output tuner and their associated assembly have been previously calibrated.

Measured load-pull results for maximum load power produced a load impedance of  $23 \Omega$ .

# CHAPTER 4

## MODELING AND EXTRACTION PROCEDURES

### 4.1 Introduction

This chapter describes the methodology of how the small-signal and large-signal model of the HEMT device is derived. Under small-signal conditions, device modeling is simplified since a linear lumped element equivalent circuit model can be easily implemented in the frequency domain. The only type of measurements necessary for the development of the linear model are DC related measurements and RF-based S-parameter measurements, which is used to extract the intrinsic elements of the small-signal model. Once the small-signal model is within tolerance of the measured S-parameter data, the optimized element values are then used in the large-signal model, along with added current sources to describe the nonlinearity in the device.

A modified version of Materka's model [Z1] was used for the large-signal model. Pulsed I-V measurements were taken at various bias levels, where the equations describing the nonlinearity of the device were then fitted to the measured data. Once the large-signal model is satisfactory and within tolerances, it can be used in a commercial high-frequency nonlinear circuit simulator to simulate the desired large-signal characterization plots such as constant gain or constant efficiency contours. The high-frequency software package that was used for the simulation of the models

in this thesis was Hewlett-Packard's Microwave Design System™. HP-Eesof's Libra also being a formidable tool.

This chapter will provide some useful information about the FET characterization, extraction, and optimization techniques that were used to create the linear and nonlinear pHEMT models. Extensive research has been done on the modeling aspect of the GaAs FET, so it is not the purpose of this thesis to improve or to delve into the intricate details of the models. The accuracy of the circuit topologies of the small-signal and large-signal models will be assumed. After an acceptable level of accuracy is found for both the small-signal and large-signal pHEMT models, nonlinear simulations of the large-signal model will be performed in order to make comparisons with the large-signal characterization measurement data of the device. The main purpose for the modeling work performed in this thesis is for the verification and comparison of the results of the load-pull measurement data with a simulation of the nonlinear model. Examination of the large-signal characterizations of the device will be explored in Chapter 5.

## 4.2 Small-Signal Modeling

To develop and create the small-signal model for the HEMT device, an extraction routine developed by Triquint's RF / Microwave Modeling Team was used [Z2]. The methodology includes an extraction process, measured data retrieval, and de-embedding. The small-signal equivalent circuit model shown in Figure 4.1 is first separated into intrinsic and extrinsic elements. For simplification purposes, the extrinsic feed networks are just displayed as blocks, although they may contain



complex structures to describe the drain, gate, and source feeds. The determination of the set of 15 parameters that characterizes the small-signal model will be briefly explained in this section.

**FIGURE 4.1:** *Small-signal pHEMT equivalent circuit model*

#### **4.2.1 Model Parameter Extraction**

The knowledge of the extrinsic resistances,  $R_G$ ,  $R_S$ , and  $R_D$ , is necessary before the extraction of the remaining 12 parameters. The component values were extracted using DC autoprobe measurements, which is taken from the GaAs front-end DC measurement system that measures Process Control Monitors during the

processing of the wafer. The values for the source and drain resistances,  $R_S$  and  $R_D$ , can be taken in such a manner. The gate resistance,  $R_G$ , can be determined from a Kelvin Measurement of the wafer. An  $R_G'$  value is constant for any model extracted from the devices on the same wafer. The value for  $R_G$  used in the model is obtained by scaling  $R_G'$  to account for the size of the gate width,  $GW$ , and the number of gate fingers,  $N$ , by using Equation 4.1 [Z1].

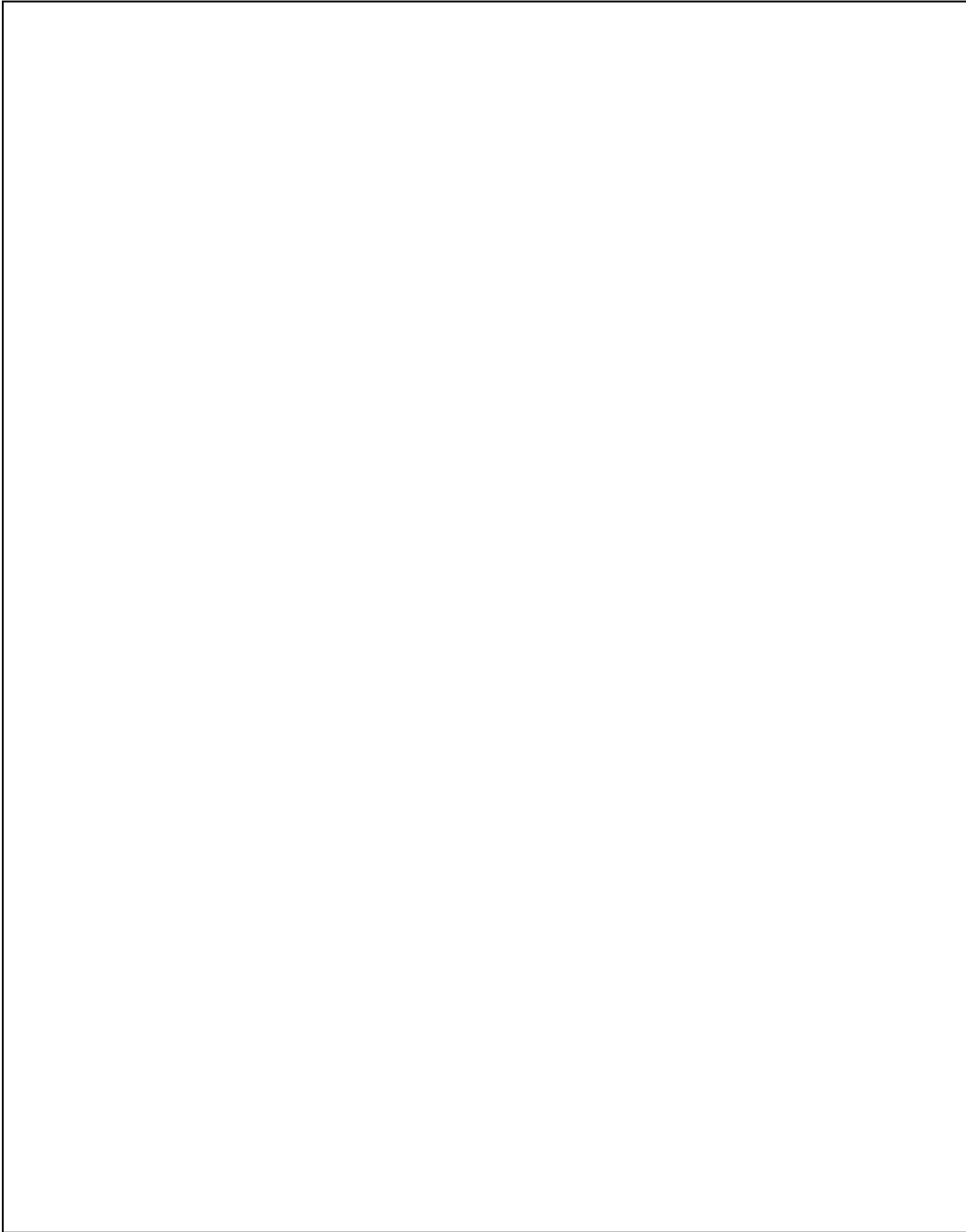
$$R_G = \frac{R_G' \cdot GW}{3 \cdot N^2} \quad (4.1)$$

Once the values for these extrinsic resistances were determined, the measured S-parameters for the device were de-embedded to the intrinsic reference plane. There are two de-embedding processes involved before the extraction routine is performed. The first process de-embeds the measured S-parameters from the measurement reference plane to the standard cell reference place using calibration standards which were specific to the particular device under test. Once completed, the second routine takes into account of the external feed structures and de-embeds the S-parameter file to the intrinsic FET reference plane. The S-parameter files used for the gate, drain, and source feed structures were modeled using HP-EEsof's Academy. Figure 5.1 depicts the reference planes of the two de-embedding processes.

Small signal data is de-embedded through the 342 um input and output transmission lines.

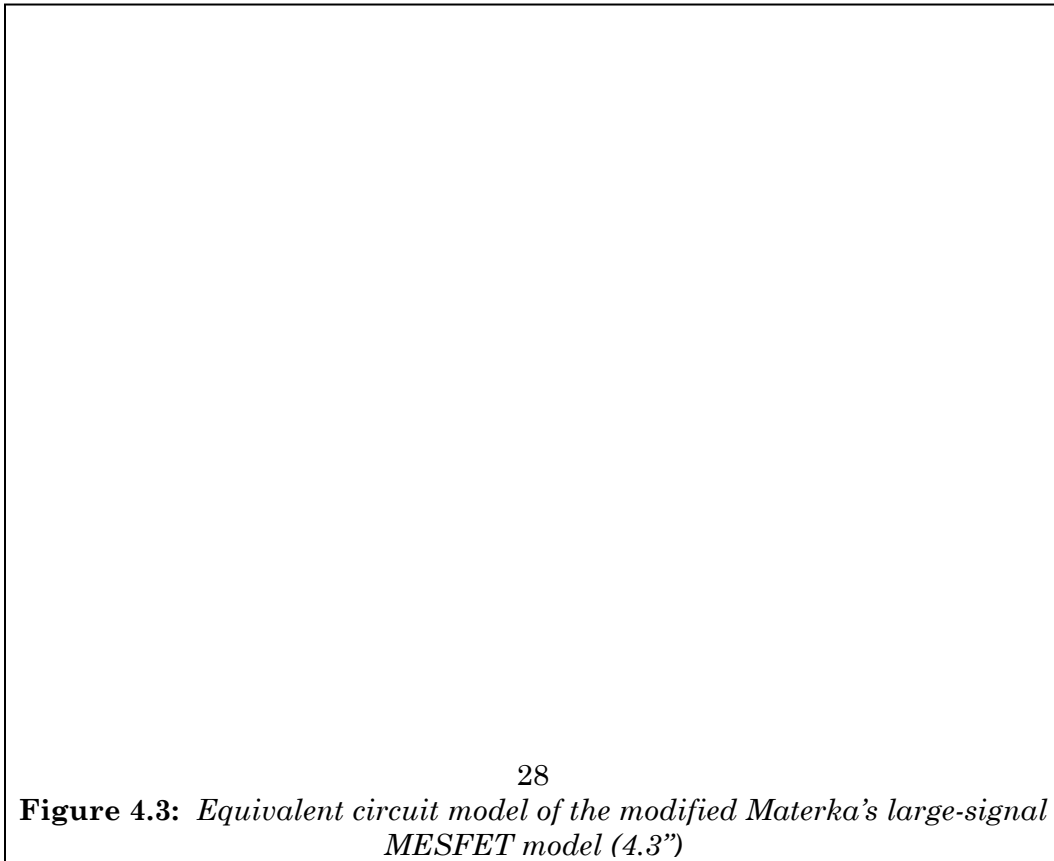
and an automated internal extraction routine is run to extract all of the circuit element values. The extraction routine uses a transcendental method to iterate to the values for the extrinsic inductances to attain the lowest overall error. The

extraction routine provides a starting point for the model parameters before optimizations are run to fit the simulated s-parameters to the measured data.



### 4.3 Large-Signal Model Formulation

The large-signal model that was used for the characterization of the FET was a modified form for the Materka-Kacprzak MESFET model [Z2]. The model, shown in Figure 5.3, has been developed by Materka and Kacprzak [Z1] to accurately characterize the nonlinear effects of the GaAs FET with the use of appropriately fitted network equations. The model was developed to decompose the circuit into a minimum number of linear and nonlinear sub-networks, using only the fitted frequency-domain parameters of the small-signal equivalent circuit to represent the linear effects of the device. The nonlinear elements of the model are described by equations which can be represented as voltage-dependent current sources across each terminal at the intrinsic reference planes.



The  $I_{GS}$  current represents the current in the gate-to-channel junction.

$$I_{GS} = I_{G0} \cdot [\exp(\alpha_G \cdot V_{GS}) - 1] \quad (4.2)$$

The  $I_{DS}$  current is described by [Z2]:

$$I_{DS} = I_{DSS} \cdot \left(1 + S_S \frac{V_{DSI}}{I_{DSS}}\right) \cdot \left[1 - \left(\frac{V_{GS}}{V_{PO} + \gamma V_{DS}}\right)\right]^{(E + KE \cdot V_{GS})} \cdot \tanh\left(\frac{S_L \cdot V_{DS}}{I_{DSS} \cdot (1 - K_G \cdot V_{GS})}\right) \quad (4.3)$$

The  $I_{GD}$  equation approximates the breakdown current and is represented by:

$$I_{GD} = I_{SR} \cdot \exp[A \cdot V_{GS} + B \cdot V_{GS}^2 + \alpha_{VB} \cdot (V_{BR} - V_{GD})] \quad (4.4)$$

To simulate the dependency of these nonlinear currents with respect to the specific intrinsic nodal voltages within MDS, a three-port Symbolically-Defined Device (SDD) was created. By using Equations 4.2 - 4.4 to model the nonlinear currents,

The model parameters within the current equations were extracted by optimizing them to fit with data taken from pulsed I-V measurements of the device. DC I-V measurements were taken on the device at 100 bias points at the Raytheon TI Systems facility, with the test setup collecting the bias voltages and currents at each port. The parameters  $I_{DSS}$ ,  $V_{PO}$ ,  $a$ , and  $g$  were optimized to fit the dc  $I_D - V_{DS}$  characteristics calculated from Equation 4.2 to the measured curve.

**Figure 4.5:** *DC I-V Plots of the Measured vs. Calculated Values ( 1 pg, 4”)*

To verify the large-signal model, it is necessary to test the consistency between the large-signal model and the small-signal model. The nonlinear model is best suited for large-signal operation but should also be able to perform accurately in the linear mode at small-signal levels. Thus to tune and create a more accurate large-signal model, small-signal s-parameters were compared between the two models over the frequency range of DC to 50 GHz. Because the intended frequency of operation for the nonlinear load-pull simulations were going to be performed at 26 GHz, there was an emphasis to create a better fit between the two models between 25 and 27 GHz. Figures [5.3] represent the comparison between the s-parameters for both the optimized small-signal and large-signal models. There seems to be very good agreement between the two models thus demonstrating the consistency of the non-linear model.



A standard cell power pHEMT device was tested and modeled for this thesis. The 300  $\mu\text{m}$  device was measured with the following bias conditions:  $\{V_{\text{DS}} = 5.0 \text{ V}; I_{\text{DS}} = 22.4 \text{ mA}; V_{\text{GS}} = 0 \text{ V}\}$ . The optimized model parameters of the device are given in Table [4.2].

**Table 4.2:** *Optimized Large-Signal Circuit Parameters (1 pg.)*

## 4.4 Conclusions

In this chapter, a small-signal and large-signal model was developed for a 300  $\mu\text{m}$  pHEMT. The models are bias-dependent and are valid over a broad frequency range from 1 to 50 GHz. An emphasis was placed upon the accuracy of the large-signal model between 25 and 27 GHz, because simulations of the load-pull characterization of the model will be performed at 26 GHz.

The small-signal model was generated using an existing MESFET circuit topology along with the extraction and “curve-fitting” of circuit element parameters using cold FET data and small-signal S-parameters. Small-signal models are generally used by universities in order to understand the transistor’s behavior and to optimize the processing to improve it. They are used in the industry mostly in order to scale devices, and to predict the RF behavior of large or smaller structures before making the processing masks [Focus App 8]. The purpose for the development the small-signal model in this thesis was to provide the internal linear components of the large-signal model.

The large-signal model was formulated using Materka’s nonlinear MESFET model with the circuit parameters derived from the linear model. The parameters for the internal nonlinear components, namely the voltage controlled current sources, were curve-fitted using Materka’s current equations and pulsed I-V data. The nonlinear model was developed to provide an accurate source to simulate a load-pull characterization of the device, which will be described in the next chapter. It is important to note, though, that in general, data provided by nonlinear models are

valid for light compression only. At 2 or 3 dB gain compression, results provided by nonlinear models can sometimes be rather inaccurate [Focus app 8].

## CHAPTER 5

# LOAD-PULL MEASUREMENTS AND SIMULATION DATA

### 5.1 Introduction

The system capabilities have been evaluated by a complete small- and large-signal characterization of a 300 nm pHEMT device produced and manufactured by Raytheon TI Systems.

### 5.3 Load-Pull Simulation Data

There are a variety of commercial microwave circuit nonlinear circuit simulators available in the market. The one that was used for the nonlinear simulations for this project was HP's Microwave Design System (MDS) software package. It was capable of simulating for the s-parameters for both the small-signal and large-signal FET model while overlaying the calculated results with the measured data. The software contains several templates that was used for the creation of simulated load-pull contours. The LoadPullCircles is a template that is included in MDS's sample design pages that generates the constant output power, load-pull circles of the amplifier under test. It is done automatically by first performing an optimization on the input and output impedances to find the maximum output power and its corresponding reflection coefficient, similar to what is performed in the actual measurement test system. The tuner is then centered at this impedance level. The angle of a second reflection coefficient term is then swept over 360 degrees, while

optimizing the magnitude of the reflection coefficient to keep the output power at a specified level below the maximum power. Thus a map of the locus of points for a specified gain can be achieved.

**Figure 5.1:** *Power Plots (1 pg.)*

**Figure 5.2:** *Load-Pull Contour Plots (1 pg.)*

The optimum region of the reflection coefficient plane for power matching is clearly seen.

## CHAPTER 6

### CONCLUSION

An L-band passive load-pull system capable for linear and nonlinear characterization of two-port transistor networks at millimeter-wave frequencies has been presented.

A load-pull measurement system can be a very efficient and accurate tool for the large-signal characterization of power amplifiers. Its main use is in the optimization of power amplifiers for radio-communication systems and radar applications.

More complete information on the non-linear behavior of GaAs MESFET's is the first and most fundamental step towards improving the power output and efficiency of solid-state power amplifiers. Two techniques for the comprehensive large-signal characterization of GaAs MESFET's have been described.

The modeling may be expanded to incorporate the simulation and measurement of harmonic power and intermodulation distortion, with the load-pull measurement system using Focus Microwave's electromechanical tuners being able to be used in any measurement system where a variable load or source impedance is required, such as, harmonic load-pull and noise-figure characterization.

# BIBLIOGRAPHY

## CHAPTER 2

Y. Takayama, "A New Load-Pull Characterization Method for Microwave Power Transistor," *Proceedings of the 1976 IEEE MTT-S Symposium Digest*, June 1976, pp. 218 - 220.

J. M. Nebus et al, "An Active Load-Pull Set-up for the Large-Signal Characterization of Highly Mismatched Microwave Power Transistors," pp. 2 - 5.

C. Tsironis, "A Computer Controlled Tuner for Accurate Oscillator Load-Pull Measurements," *Microwave Journal*, May 1992, pp. 314 - 316.

M. Pierpoint, R. D. Pollard, and J. R. Richardson, "An Automated Measurement Technique for Measuring Amplifier Load-Pull and Verifying Large-Signal Device Models," 1986 IEEE MTT-S Digest, 1986, pp. 625 - 628.

F.M

[Z1] A. Materka and T. Kacprzak, Computer Calculation of Large-Signal GaAs FET Amplifier Characteristics, *IEEE Transactions on Microwave Theory and Techniques*, February 1985, pp. 129 - 135.

[Z2] S. Skaggs, J. Gerber, G. Bilbro, and M. B. Steer, "Parameter Extraction of Microwave Transistors using a Hybrid Gradient Descent and Tree Annealing Approach," April 1993, pp. 726 - 729.

[Z2] D. R. Bridges, RF / Microwave Modeling Team Linear FET Model Extraction Methodology.

[] *Microwave Design System*, v. B.07.00, Hewlett-Packard Co.

[Z5] D. Poulin, "Load Pull - Measurement of Load Impedance of High Power Devices," p2.

[x1] Teeter

[x3] *Computer Controlled Microwave Tuner System Users Manual*, Focus Microwaves, Pointe Claire Shores, Quebec.